Intracranial glioblastoma models in preclinical neuro-oncology: neuropathological characterization and tumor progression

Marianela Candolfi, **James F. Curtin**, **W. Stephen Nichols**, **AKM. G. Muhammad**, **Gwendalyn D. King**, **G. Elizabeth Pluhar**, **Elizabeth A. McNiel**, **John R. Ohlfest**, **Andrew B. Freese**, **Peter F. Moore**, **Jonathan Lerner**, **Pedro R. Lowenstein**, and **Maria G. Castro**

M. Candolfi, J. F. Curtin, AKM.G. Muhammad, G. D. King, J. Lerner, P. R. Lowenstein, M. G. Castro, Departments of Molecular and Medical Pharmacology and Medicine, David Geffen School of Medicine, UCLA, Los Angeles, CA, USA

M. Candolfi, J. F. Curtin, G. D. King, J. Lerner, P. R. Lowenstein, M. G. Castro, Board of Governors' Gene Therapeutics Research Institute, Cedars-Sinai Medical Center, 8700 Beverly Blvd., Davis Bldg., Room 5090, Los Angeles, CA 90048, USA, e-mail: castromg@chsh.org

G. E. Pluhar, E. A. McNiel, Department of Veterinary Clinical Sciences, University of Minnesota, Saint Paul, MN, USA

J. R. Ohlfest, A. B. Freese, Department of Neurosurgery, University of Minnesota, Minneapolis, MN, USA

P. F. Moore, Department of Veterinary, Pathology, Microbiology, and Immunology, School of Veterinary Medicine, University of California, Davis, CA, USA

W. S. Nichols, Department of Pathology and Laboratory Medicine, Cedars-Sinai Medical Center, Los Angeles, CA, USA

Abstract

Although rodent glioblastoma (GBM) models have been used for over 30 years, the extent to which they recapitulate the characteristics encountered in human GBMs remains controversial. We studied the histopathological features of dog GBM and human xenograft GBM models in immune-deficient mice (U251 and U87 GBM in nude Balb/c), and syngeneic GBMs in immune-competent rodents (GL26 cells in C57BL/6 mice, CNS-1 cells in Lewis rats). All GBMs studied exhibited neovascularization, pleomorphism, vimentin immunoreactivity, and infiltration of T-cells and macrophages. All the tumors showed necrosis and hemorrhages, except the U87 human xenograft, in which the most salient feature was its profuse neovascularization. The tumors differed in the expression of astrocytic intermediate filaments: human and dog GBMs, as well as U251 xenografts expressed glial fibrillary acidic protein (GFAP) and vimentin, while the U87 xenograft and the syngeneic rodent GBMs were GFAP⁻ and vimentin⁺. Also, only dog GBMs exhibited endothelial proliferation, a key feature that was absent in the murine models. In all spontaneous and implanted GBMs we found histopathological features compatible with tumor invasion into the non-neoplastic brain parenchyma. Our data indicate that murine models of GBM appear to recapitulate several of the human GBM histopathological features and, considering their reproducibility and availability, they constitute a valuable in vivo system for preclinical studies. Importantly, our results indicate that dog GBM emerges as an attractive animal model for testing novel therapies in a spontaneous tumor in the context of a larger brain.

Correspondence to: Maria G. Castro.

Keywords

Glioma; Dog; U251; U87; CNS-1; GL26

Introduction

Glioblastoma (GBM), the most common type of primary brain tumor in adults, is a very aggressive and locally invasive tumor. Survival of patients affected by GBM has remained virtually unchanged during the last decades (i.e., 6–12 months post-diagnosis) despite advances in surgery, radiation, and chemotherapy [1-6]. The study of tumorigenesis and the evaluation of new therapies for GBM require accurate and reproducible brain tumor animal models, which ideally should recapitulate key features of the human disease, be reproducible, and resemble progression kinetics and anti-tumor immune responses of spontaneous GBM [7,8]. Although rodent glioma models have been used in preclinical glioma research for over 30 years, their use remains controversial and these models have been criticized for not recapitulating main pathological features of human GBM [9].

In vivo tumor models developed by intracranial or subcutaneous implantation of glioma cell lines in rodents are widely used to test novel therapies that target different features of GBM, i.e., angiogenesis, invasion, located within an immune privilege site (brain), secretion of immune suppressive molecules, i.e., TGFβ, amongst many others [2,3,10-12]. The advantages of these glioma models are their highly efficient gliomagenesis, reproducible growth rates, and an accurate knowledge of the location of the tumor [5]. Implantation of CNS-1 glioma cells has proved an excellent intracranial, syngeneic brain tumor model due to its high reproducibility, fast in vivo growth rates, and the absence of immunogenicity when implanted into syngeneic Lewis rats [13-15]. Human glioma xenografts implanted in immunocompromised mice are also extensively used. However, their xenogeneic nature impairs the study of immune-mediated anti-tumor strategies. Syngeneic murine models, such as GL26 mouse glioma cells in C57BL6 mice [16,17], and CNS1 rat glioma cells in Lewis rats [13-15,18] are non-immunogenic. Thus, syngeneic glioma models are excellent for studying the response of brain tumors to immunotherapy [13,14,17,19].

The lack of a large animal model of GBM had made it difficult to predict the outcome of novel therapies that have been proven successful in small rodent GBM models, when they are translated to human patients. Since dogs have larger brains than rodents, they constitute an attractive model to test novel therapeutics and optimize treatment protocols. Furthermore, brachycephalic breeds such as Boston terriers and Boxers [20-22] are predisposed to develop spontaneous GBMs that resemble the human disease [23,24]. Clinical signs and prognosis of human and canine GBMs are similar and there is a high correlation of neuroimaging features seen with MRI in canine and human GBM, which is used as a diagnostic tool for dog GBM [25,26]. Thus, dogs bearing spontaneous GBMs could constitute an attractive large animal model for GBM.

Considering the critical value of animal models in preclinical and translational cancer research, in the present work we analyzed the histological features of experimental animal models of glioma, including intracranial U251 and U87 human glioma xenografts in nude Balb/c mice, GL26 glioma cells in syngeneic C57/BL6 mice, CNS-1 glioma cells in syngeneic Lewis rats, and spontaneous GBMs in dogs, with those of the human GBM. Amongst the preclinical GBM models available we have studied the ones that are widely used by brain cancer researches, in order to better ponder the significance of our preclinical findings. The transplantation of human tumors in immune-deficient nu/nu mice gives the opportunity to assess the efficacy of therapeutic approaches in human tissues. Human xenografts have been extensively used to test

therapies that target human GBM cells, such as the fusion protein composed of IL-13 and a mutated form of Pseudomonas exotoxin (IL-13-PE). Since U251 and U87 tumors express, respectively, high and low levels of IL-13α2R (the receptor targeted by IL-13-PE), these models are very useful to test therapeutic approaches using this toxin. These models also have been used to test targeting of conditionally replicative oncolytic viruses to human GBM cells in vivo [4,27-30]. Also, the U87 model has been widely applied and proved useful when assessing GBM angiogenesis and anti-angiogenic therapeutic approaches [31-33]. However, the impairment of immune-mediated events that occur during tumorigenesis and anti-cancer therapies limits the usefulness of xenograft models. Thus, we chose a syngeneic mouse model, GL26 mouse glioma [16,34], which is non-immunogenic when injected in the brain syngeneic C57BL6 mice. This model has proven very useful for testing immunotherapeutic approaches [19]. Similarly, the CNS-1 brain tumor model was chosen because it grows well in the brain of syngeneic inbred Lewis rats [13,14]. Considering that in the rat, most glioma tumor models were derived from outbred animals, the results obtained in these models using any given immunotherapeutic strategies would be difficult to interpret. Our results indicate that murine models reproduce the histopathological features of human GBM to a greater degree than hitherto recognized, constituting valuable experimental preclinical models. Spontaneous GBMs in dogs reproduce most of the typical human GBM characteristics constitute an excellent large animal model, with therapeutic outcomes which could more closely predict their efficacy in human trials.

Materials and methods

Rodent tumor models

U251 human GBM xenografts model—U251 cells (1.5×10^6 cells in a volume of 5 μl) were implanted intracranially in the striatum of athymic Balb/c mice (NxGen BioSciences, San Diego, CA). Tumor bearing animals ($n = 10$) survived for 17–26 days (median survival 22 days).

U87 human GBM xenografts model—U87 cells (1×10^6 cells in a volume of 5 μl) were implanted intracranially in the striatum of athymic Balb/c mice (NxGen BioSciences). Tumor bearing animals ($n = 6$) had a survival of 28–29 days (median survival:28.5 days).

GL26 mouse GBM syngeneic model—About 20,000 mouse GL26 cells (0.5 μl) were implanted intracranially in the striatum of syngeneic immune-competent C57BL/6 mice (Jackson Laboratories, Bar Harbor, ME, USA). Tumor bearing mice ($n = 8$) had a survival of 26–32 days after cell implantation (median survival: 31 days).

CNS-1 rat GBM syngeneic model—About 5,000 rat CNS-1 cells (3 μl) were implanted intracranially in the striatum of syngeneic Lewis rats (220–250 g, Harlan, Indianapolis, IN, USA). Tumor bearing rats ($n = 13$) had a survival of 15–22 days (median survival:17 days).

Rodents were housed in specific pathogen free environment, and were closely monitored. Animals were housed in a humidity and temperature controlled vivarium on a 12:12 hours light/dark cycle (lights on 07:00) with free access to food and water. All experimental procedures were carried out in accordance with the NIH Guide for the Care and Use of Laboratory Animals. After anesthesia, animals were placed in a stereotactic apparatus and injected unilaterally into the right striatum. Mice were injected using 10 μl Hamilton syringe with a 33 gauge needle (coordinates: 0.5 mm forward from bregma, 2.1 mm lateral, and 3.0 mm ventral from the dura). Rats were injected using a 10 μl Hamilton syringe (coordinates: 1 mm forward from bregma, 3 mm lateral, and ventral 5 mm from the dura). Animals were allowed to recover and their health status was closely monitored. Animals were euthanized

when moribund according to the guidelines of the Institutional Animal Care and Use Committee at Cedars-Sinai Medical Center, by terminal perfusion with Tyrodes solution (132 mM NaCl, 1.8 mM $CaCl_2$, 0.32 mM NaH_2PO_4, 5.56 mM glucose, 11.6 mM $NaHCO_3$, and 2.68 mM KCl) followed by perfusion with 4% paraformaldehyde under deep anesthesia. Brains were removed, further fixed in 4% parformaldehyde and embedded in paraffin.

Human and dog spontaneous GBM

Dog GBM samples (*n* = 10) were retrieved from the archives of the School of Veterinary Sciences, University of Minnesota and human GBM samples (*n* = 5) were obtained from the archives of the Pathology Department at Cedars-Sinai Medical Center. The specimens were fixed in 10% formaldehyde and embedded in paraffin.

Histology and immunocytochemistry

Fixed tissues were dehydrated and embedded in paraffin. Tissue paraffin blocks were sectioned using a microtome. Sections of 5 μm were mounted onto slides and deparaffinized using xylene and hydrated with decreasing concentrations of ethanol. General histopathological appearance was studied in sections stained with hematoxylin and eosin (H–E). For immunocytochemical detection of astrocytic, endothelial or inflammatory markers, tissues were subjected to different protocols for antigen retrieval as described below. For all antigens, sections were incubated in the presence of 60°C preheated citrate buffer (pH 6.0) for 20 min. For F4/80, CD18, and CD3 retrieval, sections were additionally incubated with 0.05% trypsin-0.53 mM EDTA tetrasodium for 20 min at 37°C. CD68 ED1 retrieval was performed by incubating the sections with proteinase K (20 μg/ml) in TE buffer (50 mM Tris base, 1 mM EDTA tetrasodium, and pH 8.0) for 20 min at 37°C. After antigen retrieval, endogenous peroxidase was blocked with 0.3% hydrogen peroxide in PBS. Sections were then incubated with PBS containing 0.02% Triton, 0.01% Azide, and 10% fetal bovine serum to block non-specific antibody binding. Sections were incubated in the presence of primary antibodies against astrocytic intermediate filaments, including glial fibrillar astrocytic protein [anti-human glial fibrillary acidic protein (GFAP) 1:500, Chemicon, Temecula, CA] and vimentin (1:1000, Sigma, or 1:50, Abcam), and the blood vessel endothelial cell marker, Von Willebrand factor (anti-human VWF 1:50, Dako). Macrophages were identified using anti-mouse F4/80 (1:50 Serotec, Raleigh, NC) [13,35,36], anti-rat CD68 ED1 (1:1000, Serotec), anti-human CD68 (1:50, Dako), and anti-dog CD18 (1:10 developed at the Department of Veterinary, Pathology, Microbiology, and Immunology, School of Veterinary Medicine, University of California, Davis, CA) [37]. T-cells were detected using species-specific CD3 antibodies: anti-human and mouse CD3 (1:500, Dako), anti-rat CD3 (1:10, Serotec), and anti-dog CD3 (1:10 developed at the Department of Veterinary, Pathology, Microbiology, and Immunology, School of Veterinary Medicine, University of California, Davis, CA) [37]. After overnight incubation with the primary antibodies, sections were labeled with biotinylated secondary antibodies (1:1,000; Jackson Laboratory), which were detected using the Vectastain Elite ABC horseradish peroxidase method (Vector Laboratories, Burlingame, CA). After developing with diaminobenzidine (Sigma, St.Louis, MO), sections were dehydrated through graded ethanol solutions and mounted with DPX mounting media (Fluka, Sigma-Aldrich, Seelze, Germany). Tissues were analyzed and photographed using a Zeiss Axioplan microscope.

Flow cytometry

Flow cytometry was carried out as described previously [38]. Briefly, splenocytes were harvested and red blood cells were removed by incubation with ACK solution (150 mM NH_4Cl, 10 mM $KHCO_3$). Splenocytes were stained with CD3-PE (BD Pharmingen). Samples were analyzed using a FACScan flow cytometer (Beckton Dickenson, Franklin Lakes, NJ), and Summit Version 4.1 software (DAKO) was used for data analysis.

Results

In this study, we aimed to evaluate and compare the histopathological characteristics and tumor progression within the animal models commonly used for developing novel therapies for GBM. We characterized the histopathological features of transplantable, xenograft and syngeneic murine GBMs and spontaneous canine GBM, and compared them with those of GBM from human patients. To establish reproducible xenograft and syngeneic murine GBM models we injected different amounts of U251 or U87 human GBM cells in the brain of nude Balb/c mice; GL26 mouse GBM cells in the brain of syngeneic C57/B6 mice or CNS-1 rat cells in the brain of syngeneic Lewis rats. The survival of the animals was monitored for up to 2 months. The gross morphological appearance of these tumors is shown in low-magnification microphotographs in Fig. 2a. Survival curves were very reproducible in all tumor models (Fig. 2c). We found that U87 and U251 human tumors only grow to kill the host when 1,000,000 or 1,500,000 cells, respectively, are injected in the striatum of nude mice; while injecting less amount of cells does not lead to tumor grow and death of the host. Nude mice bearing U251 human tumors succumb after 17–26 days and bearing U87 human tumors after 28–29 days, with median survival of 22 and 28.6 days, respectively. In Fig. 2, we show that 20,000 GL26 cells injected in the striatum of C57/B6 mice elicit a median survival of 31 days. Injecting less amount of GL26 cells, i.e., 5,000 or 2,000, does not lead to reliable morbidity and tumor growth, with 30–70% of C57/B6 mice surviving over 60 days. Implantation of 5,000 CNS-1 cells in the striatum of Lewis rats elicits a median survival of 17 days, whilst when implanting 1,200–2,500 CNS-1 cells, the tumors do not do not grow nor induce death of the host. The main histological features of each GBM model are summarized in Table 1.

Necrosis

In Figs. 1a and 2a, low-magnification microphotographs show the gross morphological appearance of spontaneous GBMs, respectively. A characteristic feature of human GBM, i.e., presence of multiple areas of necrosis, was found in all canine GBMs. As described in the human disease [39-43], canine GBM exhibits prominent serpentine, pseudopalisading necrosis, with thrombosed tumor vessels, extensive hemorrhage, endothelial/microvascular proliferation, and high cellularity (Fig. 1a). In dog GBMs as in the human counterpart, the necrotic foci are typically surrounded by radially orientated, fusiform glioma cells in a pseudopalisading pattern (Fig. 1b).

Multiples areas of necrosis were found in all rodent GBMs, with the exception of U87 human xenografts, in which only small foci of necrosis were occasionally detected (not shown). In the syngeneic rat CNS-1 and the U251 human xenografts (Fig. 2b) necrotic foci were surrounded by radially orientated, fusiform glioma cells in a pseudopalisading pattern, although to a lesser extent than in human or dog GBM. Necrotic foci in mouse syngeneic GL26 model are surrounded by a rim of tumoral cells, which do not display the characteristic pseudopalisades (Fig. 2b). Hemorrhages, as often encountered in human GBMs [44,45], were detected in all the tumors models studied, except the U87 human xenografts. The U87 tumors were characterized by their profuse neovascularization.

Microvascular proliferation

In addition to necrosis, the presence of microvascular/endothelial proliferation (i.e., multilayered, mitotically active hyperplasic endothelial cells, smooth muscle cells, and pericytes) is a histopathological hallmark of human GBM [42-44,46,47]. Endothelial proliferation usually close to necrotic areas, with profuse vascularization was observed in dog GBMs (Fig. 1c). We did not find tumoral blood vessels exhibiting endothelial/microvascular proliferation in any of the implanted rodent GBM models.

Invasion

Tumoral cells infiltrating the normal/non-neoplastic brain parenchyma were detected in all the animal models (Figs. 3, 4). Invasion in dog GBM was characterized by widespread tumoral cells within the non-neoplastic brain parenchyma. As in the human GBM specimens (Fig. 3b), we found abundant cells migrating into the white matter and surrounding neurons and blood vessels (Fig. 3a). Since it is difficult to determine whether the cells that infiltrate the non-neoplastic brain parenchyma are tumoral or inflammatory cells, we stained dog and human GBM sections with GFAP antibodies and counterstained them with eosin. We found small rounded cells with abnormal cytoplasmic and nuclear morphology infiltrating the non-neoplastic brain parenchyma expressing GFAP, which is suggestive of their glial origin (Fig. 3).

In the murine GBM models tumor cells infiltrating the non-neoplastic brain parenchyma were identified by their strongly acidophilic cytoplasm, their high nucleus to cytoplasm ratio, nuclear and cytoplasmic abnormal morphology, and their pleomorphism (Fig. 4). Peritumoral infiltration of the brain parenchyma was detected around the tumor, although the tumor borders in the rodent models are not as diffuse as those of the spontaneous GBM in dog and human. Scattered tumor cells and aggregates were also detected within the white matter tracts, as reported in human GBM, and abnormal blood vessels were encountered in the rodent brain (Fig. 4). We measured the distance between the tumor borders and the tumor cells or aggregates that infiltrate the normal brain parenchyma. The median and maximum distances between the tumor border and the cells infiltrating the normal parenchyma were as follow: U251 tumors: median 580 μ, maximum 850 μ; U87 tumors: median 180 μ, maximum 250 μ; GL26 tumors: median 250 μ, maximum 660 μ; CNS-1 tumors: median 470 μ, maximum 640 μ.

Cellular composition of GBMs

All GBMs exhibited hypercellularity, nuclear atypia, and pleomorphism, including multinucleated giant cells (Fig. 5a). Aberrant mitotic figures were readily observed. Canine GBMs were usually composed of small anaplastic cells. Although poorly differentiated cells were found in all GBMs, they expressed astrocytic intermediate filaments. Considering that there is no specific marker for GBM cells, we assessed the expression of proteins that are expressed in reactive astrocytes. In the adult brain, astrocytes contain two types of intermediate filaments: vimentin positive filaments and GFAP positive filaments. Although vimentin is expressed also in blood vessels and ependymal cells, in the brain parenchyma vimentin is not expressed in neurons or any other subclass of glial cell other than reactive astrocytes [48]. Thus, although vimentin expression is not exclusive to astrocytes, its expression, together with GFAP in these tumors is suggestive of their glial origin. The expression of GFAP is variable in human GBM [49] and depends on the degree of anaplasia. While usually only cells with astrocytic morphology are positive for GFAP, vimentin staining is more widespread throughout the tumors [50]. In dog GBMs, the GFAP staining pattern was similar to that of the human tumors, exhibiting positive stained cells with astrocytic shape and small rounded GFAP negative cells (Fig. 5c). GFAP staining was also detected in U251 human xenografts, while the U87 human xenograft and the syngeneic murine GBMs were negative for GFAP. However, homogeneous vimentin staining was observed in all the GBMs studied, i.e., rodent models, spontaneous dog GBMs (Fig. 5b). Similarly to human GBMs [43-45,51], spontaneous and implanted GBM models were highly vascularized, as shown by Von Willebrand factor staining of endothelial cells (Fig. 5d). The U87 human xenografts were the implanted GBM model that showed the most profuse vascularization.

Inflammatory cells' infiltration

Macrophage and T-cell infiltration has been reported in human GBMs [52]. As shown in Fig. 6 abundant infiltration of these inflammatory/immune cells was also observed in the canine

GBM and all the murine tumor models. Surprisingly, we detected not only heavy macrophage infiltration, but also CD3^{+} lymphocytes infiltrating U251 and U87 human GBM xenografts in nude mice, although to a lesser extent than in the immuno-competent syngeneic murine models. We used flow cytometry to confirm the existence of CD3^{+} lymphocytes in the spleens of the nude mice and wild type mice. In agreement with our immunohistochemical analysis of tumors, we identified CD3^{+} cells in the spleens of nude mice, albeit at a much lower total number compared with wild type mice (nu/nu Balb/c: 9% ± 2.1 CD3^{+} splenocytes; wild type C57/B6: 22% ± 3.6 CD3^{+} splenocytes).

Discussion

Rodent models of GBM have been used for more than 30 years, in spite of this; their histological features have been poorly characterized in relation to spontaneous GBMs. Moreover, the translational potential of rodent GBM models to develop novel therapeutic approaches for human GBM is still a matter of debate [9]. Ideally, brain tumor models should be of glial origin, grow in vitro and in vivo with predictable and reproducible growth patterns, have close resemblance in vivo to the histopathology of human gliomas, be weakly or non-immunogenic, and ultimately, their progression in vivo should be highly reproducible. Unfortunately, the ideal GBM animal model that comprises all of the above features does not exist. Thus, it is essential to identify the strengths and weaknesses of different available tumor models in order to select the most appropriate GBM model depending upon the nature of the study to be conducted. In this paper, we report histopathological results after a comprehensive characterization of commonly used xenografts and syngeneic murine intracranial GBM models and spontaneous canine GBM. The main histological and biological features of each GBM model are summarized in Tables 1 and 2, respectively.

The availability of a number of genetically engineered immuno-supressed rodents has allowed the development of human GBM tumors as intracranial or subcutaneous xenograft in vivo models [53,54]. Although these models have been criticized for not reproducing the tumor-host immune system interactions and for not accurateely representing the cellular composition of the original tumors [9], they have also proved very useful in preclinical research. These models have been also criticized by their low and variable tumor formation rate [9]. In the present work, we injected $1–1.5 \times 10^6$ cells to reproducibly induce tumor growth in the xenograph models in nude mice, while syngeneic rodent models only require 5,000–20,000 cells to grow in the brain. This difference in the amount of cells required to develop intracranial tumors suggests that human glioma cells have lower ability to grow in the mouse brain than rodent glioma cells, or, alternatively, that the immune response to xenotransplants is not completely abolished in nude mice. To evaluate this possibility, we characterized immune cells infiltrating the U251 and U87 human GBM xenografts in the brains of the athymic nu/nu Balb/c mice. In accordance with previous reports [55-57], we also found CD3^{+} lymphocytes in the spleens of nude mice. In fact, mature CD3^{+} T-cells capable of activation have been reported in the skin [58,59], blood and lymph nodes [60], gut [61], and spleen [62] of athymic mice, the extrathymic site for T-cells maturation remains under investigation. These models allow studying the response of human GBM tissue in the context of normal brain tissue. Also the U251 xenograft GBM tumor exhibits histological features that are similar to those of the human GBM, including the presence of necrosis, angiogenesis, and tumoral cell infiltration as well as the astrocytic phenotype (Table 1). Although U87 GBM tumors fail to resemble the necrotic foci of the human tumors and their invasion pattern is less aggressive than the U251 tumor, they exhibit profuse angiogenesis, which allows testing therapeutic approaches that target neovascularization [31,63]. The U87 human xenograft model was the most profusely vascularized tumor amongst the rodent models, followed by the U251 human xenograft, both of which express VEGF [64]. However, neovascularization observed in the rodent GBM models was phenotypically distinct from the human GBM. Although it has been shown that

U87 cells can induce endothelial cell proliferation in vitro [63], the absence of endothelial proliferation in U87 tumors in vivo could be due to the fast kinetics of tumor development in rodent models compared to spontaneous GBM in dogs or humans. This could also be a result of the lack of extracellular matrix components involved in endothelial cell migration and proliferation in the murine host [65-67]. Nevertheless, these models has been widely applied and proved useful when assessing GBM angiogenesis and anti-angiogenic therapeutic approaches [31-33]. Moreover, recent evidence shows that human xenografts retain GBM gene amplifications detected in the in situ tumors [68,69]. Intracranial human GBM xenograft models have also proved very useful in the evaluation of new diagnostic imaging techniques [70], as well as in the preclinical research of novel anti-tumoral approaches involving chemotherapy [71], radiotherapy [72], targeted toxins [73], cytotoxic [74] or conditionally replicative oncolytic viruses [27-30,75].

The syngeneic experimental models of glioma which we studied in this paper all share some of the characteristic neuropathological features with human GBM. Although the anatomical invasion pattern of the syngeneic murine models differs from that of the human GBM, tumoral cells were readily encountered infiltrating non-neoplastic tissue surrounding the tumors. In addition, the syngeneic rodent GBM models are technically easy to develop and very reproducible [13-15,18,19,76]. The accessibility of wild type mice and rats also make them a useful first screening model for novel therapies in vivo. Since these animals have an intact immune system, they are suitable to test therapies that enhance the host immune response against the tumor [13,14].

We previously used the CNS-1 syngeneic tumor model to test the efficacy of a gene therapy approach that combines the cytotoxic properties of HSV1-TK [77,78] with the immunostimulatory effects of Flt3L [13,14,38], which is also successful when tested in the GL26 intracranial tumor model [17]. In another study, GL26 intracranial tumors were treated with an immunotherapeutic approach that elicits glioma tumor-specific cytotoxic T lymphocytes induced by vaccination using dendritic cells engineered to express IL-12 [19]. Thus, these syngeneic GBM models in rodents constitute excellent in vivo systems for the preclinical testing of novel immune-therapeutic strategies.

We found that the rodent models of GBM exhibit histopathological features compatible with tumor invasion into the non-neoplastic brain parenchyma. However, the level of invasion in the rodent models is both qualitatively and quantitatively different than in humans, with invasion in the rodent models limited to less than 1mm from the tumor mass. The clinical relevance of these feature relies in the fact that post-resection recurrences of GBM occur most often in the immediate vicinity of the resected tumor mass [79,80]. On the other hand, a novel model recently described closely resembles the invasive pattern of the human GBM [81]. In this model, overexpression of PDGF in the adult rat white matter led to invasive tumors that grew to kill the hosts in 2–3 weeks.

Dogs bearing induced or spontaneous tumors, including breast [82], prostate [83], lung [84], and lymphohematopoietic [85] neoplasms have already being proposed as excellent animal models [86]. The presence of pseudopalisading necrosis and endothelial proliferation that closely resemble those found in human GBMs suggest the presence of a hypoxic environment in dog GBM, as described in humans [39-41]. Among the tumor models studied in this paper, the spontaneous dog GBM is the only one that exhibits endothelial proliferation. Importantly, we show that canine GBM is highly invasive, exhibiting the classical patterns of human GBM invasion, which is characterized by the diffuse spread of tumoral cells within the non-neoplastic brain parenchyma [7,43-45,51]. This feature of dog GBM makes it the only large animal model available, to accurately reproduce the invasive behavior of human GBM. The latter is very

important when testing not only the efficacy of novel therapies, but also their toxicity to the normal brain.

The large size of the dog brain, compared to the rodent one, would be more useful for preclinical assessment of doses and volumes needed to implement novel therapies. Also, the detection of therapy-induced toxicity and side effects, as well as behavioral abnormalities is very developed in dogs, since they are routinely assessed clinically by veterinarians. Moreover, the individual variability of outbreed dogs will help to better predict the clinical outcomes in human patients. However, the spontaneous GBM in dog is not a tumor model as easily available as the rodent GBM models. Nevertheless, the feasibility of using this spontaneous GBM model is facilitated by the possibility of recruiting GBM bearing dogs from Veterinary Hospitals. GBM is the most common primary brain tumor in dogs, and brachycephalic breeds such as Boston terriers and Boxers, are genetically predisposed to develop these tumors [20-22]. A detailed retrospective search for canine brain tumor cases seen at the University of Minnesota showed that from January 1, 2003 to December 31, 2005 there were 110 canine cases of brain tumors, which definitive diagnoses or tentative diagnoses based on CT imaging were as follows: glioma— 48; pituitary—20 (suspected to be macro-adenoma); meningioma—20; lymphoma—3; spindle cell sarcoma—1; open diagnosis—18. These numbers of cases were found without any specific case solicitation and only taking into account cases that had CT imaging of the brain. Thus, based on this retrospective clinical search, the Veterinary. School at The University of Minnesota routinely admits at least four dogs per month with a newly diagnosed brain tumor without any specific announcements for clinical trial recruitment; ~40–45% are diagnosed as glioma based on imaging studies. This suggests that an average of 18–20 dogs per year could be recruited for an efficacy clinical trial of novel therapies against GBM.

In summary, our report indicates that xenograft and syngenic mouse and rat models share histopathological characteristics with human GBM to a greater degree than hitherto recognized. Therefore, considering their reproducibility, inexpensiveness and availability, they constitute good preclinical models to test the efficacy and putative side effects of novel therapies. Spontaneous GBMs in dogs reproduce most typical human GBM characteristics and constitute an excellent large animal model for GBM, which could better predict the effectiveness of novel therapeutic approaches in human trials.

References

1. Castro MG, Cowen R, Williamson IK, David A, Jimenez-Dalmaroni MJ, Yuan X, Bigliari A, Williams JC, Hu J, Lowenstein PR. Current and future strategies for the treatment of malignant brain tumors. Pharmacol Ther 2003;98:71–108. [PubMed: 12667889]

2. Chiocca EA. Oncolytic viruses. Nat Rev Cancer 2002;2:938–950. [PubMed: 12459732]

3. Curtin JF, King GD, Candolfi M, Greeno RB, Kroeger KM, Lowenstein PR, Castro MG. Combining cytotoxic and immune-mediated gene therapy to treat brain tumors. Curr Top Med Chem 2005;5:1151–1170. [PubMed: 16248789]

4. Gomez-Manzano C, Yung WK, Alemany R, Fueyo J. Genetically modified adenoviruses against gliomas: from bench to bedside. Neurology 2004;63:418–426. [PubMed: 15304571]

5. King GD, Curtin JF, Candolfi M, Kroeger K, Lowenstein PR, Castro MG. Gene therapy and targeted toxins for glioma. Curr Gene Ther 2005;5:535–557. [PubMed: 16457645]

6. Prados MD, Levin V. Biology and treatment of malignant glioma. Semin Oncol 2000;27:1–10. [PubMed: 10866344]

7. Maher EA, Furnari FB, Bachoo RM, Rowitch DH, Louis DN, Cavenee WK, DePinho RA. Malignant glioma: genetics and biology of a grave matter. Genes Dev 2001;15:1311–1333. [PubMed: 11390353]

8. Kleihues P, Zulch KJ, Matsumoto S, Radke U. Morphology of malignant gliomas induced in rabbits by systemic application of N-methyl-N-nitrosourea. Z Neurol 1970;198:65–78. [PubMed: 4100120]

9. Ding H, Nagy A, Gutmann DH, Guha A. A review of astrocytoma models. Neurosurg Focus 2000;8:1–8.

10. Castro, MG.; Curtin, J.; King, GD.; Candolfi, M.; Czer, P.; Sciascia, S.; Kroeger, K.; Fakhouri, T.; Honig, S.; Kuoy, W.; Kang, T.; Johnson, S.; Lowenstein, PR. Novel gene therapeutic approaches to brain cancer. In: Castro, MG.; Lowenstein, PR., editors. Gene therapy for neurological disorders. Taylor and Francis Group; New York: 2006. p. 229-264.

11. Fecci PE, Mitchell DA, Archer GE, Morse MA, Lyerly HK, Bigner DD, Sampson JH. The history, evolution, and clinical use of dendritic cell-based immunization strategies in the therapy of brain tumors. J Neurooncol 2003;64:161–176. [PubMed: 12952297]

12. Rainov NG, Ren H. Gene therapy for human malignant brain tumors. Cancer J 2003;9:180–188. [PubMed: 12952303]

13. Ali S, Curtin JF, Zirger JM, Xiong W, King GD, Barcia C, Liu C, Puntel M, Goverdhana S, Lowenstein PR, Castro MG. Inflammatory and anti-glioma effects of an adenovirus expressing human soluble Fms-like tyrosine kinase 3 ligand (hsFlt3L): treatment with hsFlt3L inhibits intracranial glioma progression. Mol Ther 2004;10:1071–1084. [PubMed: 15564139]

14. Ali S, King GD, Curtin JF, Candolfi M, Xiong W, Liu C, Puntel M, Cheng Q, Prieto J, Ribas A, Kupiec-Weglinski J, van Rooijen N, Lassmann H, Lowenstein PR, Castro MG. Combined immunostimulation and conditional cytotoxic gene therapy provide long-term survival in a large glioma model. Cancer Res 2005;65:7194–7204. [PubMed: 16103070]

15. Kruse CA, Molleston MC, Parks EP, Schiltz PM, Kleinschmidt-DeMasters BK, Hickey WF. A rat glioma model, CNS-1, with invasive characteristics similar to those of human gliomas: a comparison to 9L gliosarcoma. J Neurooncol 1994;22:191–200. [PubMed: 7760095]

16. Albright L, Madigan JC, Gaston MR, Houchens DP. Therapy in an intracerebral murine glioma model, using Bacillus Calmette-Guerin, neuraminidase-treated tumor cells, and 1-(2-chloroethyl)-3-cyclohexyl-1-nitrosourea. Cancer Res 1975;35:658–665. [PubMed: 234790]

17. Curtin J, King GD, Xiong W, Liu C, Lowenstein PR, Castro MG. Stimulation of the immune system using gene therapy is an effective approach for treating brain tumors in mouse and rat models. American society of gene therapy 8th annual meeting. Mol Ther 2005;11:S106.

18. Owens GC, Orr EA, DeMasters BK, Muschel RJ, Berens ME, Kruse CA. Overexpression of a transmembrane isoform of neural cell adhesion molecule alters the invasiveness of rat CNS-1 glioma. Cancer Res 1998;58:2020–2028. [PubMed: 9581848]

19. Kim CH, Hong MJ, Park SD, Kim CK, Park MY, Sohn HJ, Cho HI, Kim TG, Hong YK. Enhancement of anti-tumor immunity specific to murine glioma by vaccination with tumor cell lysate-pulsed dendritic cells engineered to produce interleukin-12. Cancer Immunol Immunother 2006;55:1309–1319. [PubMed: 16463038]

20. Heidner GL, Kornegay JN, Page RL, Dodge RK, Thrall DE. Analysis of survival in a retrospective study of 86 dogs with brain tumors. J Vet Intern Med 1991;5:219–226. [PubMed: 1941756]

21. Foster ES, Carrillo JM, Patnaik AK. Clinical signs of tumors affecting the rostral cerebrum in 43 dogs. J Vet Intern Med 1988;2:71–74. [PubMed: 3221360]

22. LeCouteur RA. Current concepts in the diagnosis and treatment of brain tumours in dogs and cats. J Small Anim Pract 1999;40:411–416. [PubMed: 10516946]

23. Stonehewer J, Mackin AJ, Tasker S, Simpson JW, Mayhew IG. Idiopathic phenobarbital-responsive hypersialosis in the dog: an unusual form of limbic epilepsy? J Small Anim Pract 2000;41:416–421. [PubMed: 11023129]

24. Stoica G, Kim HT, Hall DG, Coates JR. Morphology, immunohistochemistry, and genetic alterations in dog astrocytomas. Vet Pathol 2004;41:10–19. [PubMed: 14715963]

25. Lipsitz D, Higgins RJ, Kortz GD, Dickinson PJ, Bollen AW, Naydan DK, LeCouteur RA. Glioblastoma multiforme: clinical findings, magnetic resonance imaging, and pathology in five dogs. Vet Pathol 2003;40:659–669. [PubMed: 14608019]

26. Orrison WW Jr, Rose DF, Hart BL, Maclin EL, Sanders JA, Willis BK, Marchand EP, Wood CC, Davis LE. Noninvasive preoperative cortical localization by magnetic source imaging. AJNR Am J Neuroradiol 1992;13:1124–1128. [PubMed: 1636523]

27. Aghi M, Rabkin S, Martuza RL. Effect of chemotherapy-induced DNA repair on oncolytic herpes simplex viral replication. J Natl Cancer Inst 2006;98:38–50. [PubMed: 16391370]

28. Conrad C, Miller CR, Ji Y, Gomez-Manzano C, Bharara S, McMurray JS, Lang FF, Wong F, Sawaya R, Yung WK, Fueyo J. Delta24-hyCD adenovirus suppresses glioma growth in vivo by combining oncolysis and chemosensitization. Cancer Gene Ther 2005;12:284–294. [PubMed: 15650766]

29. Jiang H, Gomez-Manzano C, Alemany R, Medrano D, Alonso M, Bekele BN, Lin E, Conrad CC, Yung WK, Fueyo J. Comparative effect of oncolytic adenoviruses with E1A-55 kDa or E1B-55 kDa deletions in malignant gliomas. Neoplasia 2005;7:48–56. [PubMed: 15720816]

30. Samoto K, Ehtesham M, Perng GC, Hashizume K, Wechsler SL, Nesburn AB, Black KL, Yu JS. A herpes simplex virus type 1 mutant with gamma 34.5 and LAT deletions effectively oncolyses human U87 glioblastomas in nude mice. Neurosurgery 2002;50:599–605. [PubMed: 11841729]discussion 605–606

31. Kirsch M, Strasser J, Allende R, Bello L, Zhang J, Black PM. Angiostatin suppresses malignant glioma growth in vivo. Cancer Res 1998;58:4654–4659. [PubMed: 9788618]

32. Lund EL, Bastholm L, Kristjansen PE. Therapeutic synergy of TNP-470 and ionizing radiation: effects on tumor growth, vessel morphology, and angiogenesis in human glioblastoma multiforme xenografts. Clin Cancer Res 2000;6:971–978. [PubMed: 10741723]

33. Schmidt NO, Ziu M, Carrabba G, Giussani C, Bello L, Sun Y, Schmidt K, Albert M, Black PM, Carroll RS. Antiangiogenic therapy by local intracerebral microinfusion improves treatment efficiency and survival in an orthotopic human glioblastoma model. Clin Cancer Res 2004;10:1255–1262. [PubMed: 14977823]

34. Ausman JI, Shapiro WR, Rall DP. Studies on the chemotherapy of experimental brain tumors: development of an experimental model. Cancer Res 1970;30:2394–2400. [PubMed: 5475483]

35. Kosugi I, Kawasaki H, Arai Y, Tsutsui Y. Innate immune responses to cytomegalovirus infection in the developing mouse brain and their evasion by virus-infected neurons. Am J Pathol 2002;161:919–928. [PubMed: 12213720]

36. Chen SC, Leach MW, Chen Y, Cai XY, Sullivan L, Wiekowski M, Dovey-Hartman BJ, Zlotnik A, Lira SA. Central nervous system inflammation and neurological disease in transgenic mice expressing the CC chemokine CCL21 in oligodendrocytes. J Immunol 2002;168:1009–1017. [PubMed: 11801633]

37. Stein VM, Czub M, Schreiner N, Moore PF, Vandevelde M, Zurbriggen A, Tipold A. Microglial cell activation in demyelinating canine distemper lesions. J Neuroimmunol 2004;153:122–131. [PubMed: 15265670]

38. Curtin JF, King GD, Barcia C, Liu C, Hubert FX, Guillonneau C, Josien R, Anegon I, Lowenstein PR, Castro MG. Fms-like tyrosine kinase 3 ligand recruits plasmacytoid dendritic cells to the brain. J Immunol 2006;176:3566–3577. [PubMed: 16517725]

39. Brat DJ, Castellano-Sanchez AA, Hunter SB, Pecot M, Cohen C, Hammond EH, Devi SN, Kaur B, Van Meir EG. Pseudopalisades in glioblastoma are hypoxic, express extracellular matrix proteases, and are formed by an actively migrating cell population. Cancer Res 2004;64:920–927. [PubMed: 14871821]

40. Dong S, Nutt CL, Betensky RA, Stemmer-Rachamimov AO, Denko NC, Ligon KL, Rowitch DH, Louis DN. Histology-based expression profiling yields novel prognostic markers in human glioblastoma. J Neuropathol Exp Neurol 2005;64:948–955. [PubMed: 16254489]

41. Rong Y, Durden DL, Van Meir EG, Brat DJ. 'Pseudopalisading' necrosis in glioblastoma: a familiar morphologic feature that links vascular pathology, hypoxia, and angiogenesis. J Neuropathol Exp Neurol 2006;65:529–539. [PubMed: 16783163]

42. Maher, E.; McKee, A. Neoplasms of the central nervous system. In: Skarin, A., III, editor. Atlas of diagnostic oncology. Elsevier; Amsterdam: 2003.

43. Frosch, M.; Anthony, D.; Girolami, D. The central nervous system. In: Kumar, V.; Abbas, A.; Fausto, N., editors. Robbins and cotran pathologic basis of disease. Elsevier; Amsterdam: 2005.

44. Fine, H.; Barker, F.; Market, J.; Loeffer, J. Neoplasms of the central nervous system. In: Vita, VD., VII; Rosenberg, S.; Hellman, S., editors. Cancer principles and practice of oncology. Lippincott; Philadelphia: 2005.

45. Trojanoski, J. The nervous system. In: Rubin, E., IV, et al., editors. Rubin's pathology. Clinopathologic foundations of medicine. Lippincott; Philadelphia: 2005.

46. Fischer I, Gagner JP, Law M, Newcomb EW, Zagzag D. Angiogenesis in gliomas: biology and molecular pathophysiology. Brain Pathol 2005;15:297–310. [PubMed: 16389942]

47. Zagzag D, Friedlander DR, Margolis B, Grumet M, Semenza GL, Zhong H, Simons JW, Holash J, Wiegand SJ, Yancopoulos GD. Molecular events implicated in brain tumor angiogenesis and invasion. Pediatr Neurosurg 2000;33:49–55. [PubMed: 11025423]

48. Schnitzer J, Franke WW, Schachner M. Immunocytochemical demonstration of vimentin in astrocytes and ependymal cells of developing and adult mouse nervous system. J Cell Biol 1981;90:435–447. [PubMed: 7026573]

49. Jones TR, Bigner SH, Schold SC Jr, Eng LF, Bigner DD. Anaplastic human gliomas grown in athymic mice. Morphology and glial fibrillary acidic protein expression. Am J Pathol 1981;105:316–327. [PubMed: 6274201]

50. Elison, D.; Love, S.; Chimelli, L.; Lowe, K.; Roberts, GW.; Vinters, HV. Astrocytic neoplasms. In: Ellison, D.; Love, S., editors. Neuropathology. Mosby International Ltd.; Barcelona, Spain: 1998. p. 35.1-35.10.

51. Kleihues, P.; Burger, P.; Collins, V. Glioblastoma. In: Kleihues, P., II; Cavenee, WK., editors. Pathology and genetics of the nervous system. International Agency for Research on Cancer; Lyon, France: 2000. p. 29-39.

52. Leung SY, Wong MP, Chung LP, Chan AS, Yuen ST. Monocyte chemoattractant protein-1 expression and macrophage infiltration in gliomas. Acta Neuropathol (Berl) 1997;93:518–527. [PubMed: 9144591]

53. Horten BC, Basler GA, Shapiro WR. Xenograft of human malignant glial tumors into brains of nude mice. A histopatholgical study. J Neuropathol Exp Neurol 1981;40:493–511. [PubMed: 7276991]

54. Jones NR, Rossi ML, Gregoriou M, Hughes JT. Investigation of the expression of epidermal growth factor receptor and blood group A antigen in 110 human gliomas. Neuropathol Appl Neurobiol 1990;16:185–192. [PubMed: 2402328]

55. Benveniste P, Chadwick BS, Miller RG, Reimann J. Characterization of cells with T cell markers in athymic nude bone marrow and of their in vitro-derived clonal progeny. Comparison with euthymic bone marrow. J Immunol 1990;144:411–419. [PubMed: 2136889]

56. Palacios R, Samaridis J. Rearrangement patterns of T-cell receptor genes in the spleen of athymic (nu/nu) young mice. Immunogenetics 1991;33:90–95. [PubMed: 1999354]

57. Takigawa M, Hanaoka M. In vivo maturation of B cells in the spleen of nude mice following administration of bacterial lipopolysaccharide. Int Arch Allergy Appl Immunol 1978;56:115–122. [PubMed: 340388]

58. Payer E, Strohal R, Kutil R, Elbe A, Stingl G. Demonstration of a CD3+ lymphocyte subset in the epidermis of athymic nude mice. Evidence for T cell receptor diversity. J Immunol 1992;149:413–420. [PubMed: 1352529]

59. Shiohara T, Moriya N, Hayakawa J, Arahari K, Yagita H, Nagashima M, Ishikawa H. Bone marrow-derived dendritic epidermal T cells express T cell receptor-alpha beta/CD3 and CD8. Evidence for their extrathymic maturation. J Immunol 1993;150:4323–4330. [PubMed: 8097753]

60. Kennedy JD, Pierce CW, Lake JP. Extrathymic T cell maturation. Phenotypic analysis of T cell subsets in nude mice as a function of age. J Immunol 1992;148:1620–1629. [PubMed: 1347303]

61. Bandeira A, Itohara S, Bonneville M, Burlen-Defranoux O, Mota-Santos T, Coutinho A, Tonegawa S. Extrathymic origin of intestinal intraepithelial lymphocytes bearing T-cell antigen receptor gamma delta. Proc Natl Acad Sci USA 1991;88:43–47. [PubMed: 1986381]

62. Kirk SJ, Regan MC, Wasserkrug HL, Sodeyama M, Barbul A. Arginine enhances T-cell responses in athymic nude mice. JPEN J Parenter Enteral Nutr 1992;16:429–432. [PubMed: 1433776]

63. Bello L, Lucini V, Giussani C, Carrabba G, Pluderi M, Scaglione F, Tomei G, Villani R, Black PM, Bikfalvi A, Carroll RS. IS20I, a specific alphavbeta3 integrin inhibitor, reduces glioma growth in vivo. Neurosurgery 2003;52:177–185. [PubMed: 12493116]discussion 185–186

64. Ke LD, Shi YX, Im SA, Chen X, Yung WK. The relevance of cell proliferation, vascular endothelial growth factor, and basic fibroblast growth factor production to angiogenesis and tumorigenicity in human glioma cell lines. Clin Cancer Res 2000;6:2562–2572. [PubMed: 10873113]

65. Hornebeck W, Emonard H, Monboisse JC, Bellon G. Matrix-directed regulation of pericellular proteolysis and tumor progression. Semin Cancer Biol 2002;12:231–241. [PubMed: 12083853]

66. Taipale J, Saharinen J, Keski-Oja J. Extracellular matrix-associated transforming growth factor-beta: role in cancer cell growth and invasion. Adv Cancer Res 1998;75:87–134. [PubMed: 9709808]

67. Wickstrom SA, Alitalo K, Keski-Oja J. Endostatin signaling and regulation of endothelial cell-matrix interactions. Adv Cancer Res 2005;94:197–229. [PubMed: 16096002]

68. Giannini C, Sarkaria JN, Saito A, Uhm JH, Galanis E, Carlson BL, Schroeder MA, James CD. Patient tumor EGFR and PDGFRA gene amplifications retained in an invasive intracranial xenograft model of glioblastoma multiforme. Neuro-oncol 2005;7:164–176. [PubMed: 15831234]

69. Sarkaria JN, Carlson BL, Schroeder MA, Grogan P, Brown PD, Giannini C, Ballman KV, Kitange GJ, Guha A, Pandita A, James CD. Use of an orthotopic xenograft model for assessing the effect of epidermal growth factor receptor amplification on glioblastoma radiation response. Clin Cancer Res 2006;12:2264–2271. [PubMed: 16609043]

70. Cho SY, Ravasi L, Szajek LP, Seidel J, Green MV, Fine HA, Eckelman WC. Evaluation of (76)Br-FBAU as a PET reporter probe for HSV1-tk gene expression imaging using mouse models of human glioma. J Nucl Med 2005;46:1923–1930. [PubMed: 16269608]

71. Tentori L, Leonetti C, Scarsella M, D'Amati G, Vergati M, Portarena I, Xu W, Kalish V, Zupi G, Zhang J, Graziani G. Systemic administration of GPI 15427, a novel poly(ADP-ribose) polymerase-1 inhibitor, increases the antitumor activity of temozolomide against intracranial melanoma, glioma, lymphoma. Clin Cancer Res 2003;9:5370–5379. [PubMed: 14614022]

72. Shen S, Khazaeli MB, Gillespie GY, Alvarez VL. Radiation dosimetry of 131I-chlorotoxin for targeted radiotherapy in glioma-bearing mice. J Neurooncol 2005;71:113–119. [PubMed: 15690125]

73. Kawakami K, Kawakami M, Kioi M, Husain SR, Puri RK. Distribution kinetics of targeted cytotoxin in glioma by bolus or convection-enhanced delivery in a murine model. J Neurosurg 2004;101:1004–1011. [PubMed: 15597761]

74. Cirielli C, Inyaku K, Capogrossi MC, Yuan X, Williams JA. Adenovirus-mediated wild-type p53 expression induces apoptosis and suppresses tumorigenesis of experimental intracranial human malignant glioma. J Neurooncol 1999;43:99–108. [PubMed: 10533721]

75. Lamfers ML, Gianni D, Tung CH, Idema S, Schagen FH, Carette JE, Quax PH, Van Beusechem VW, Vandertop WP, Dirven CM, Chiocca EA, Gerritsen WR. Tissue inhibitor of metalloproteinase-3 expression from an oncolytic adenovirus inhibits matrix metalloproteinase activity in vivo without affecting antitumor efficacy in malignant glioma. Cancer Res 2005;65:9398–9405. [PubMed: 16230403]

76. Dewey RA, Morrissey G, Cowsill CM, Stone D, Bolognani F, Dodd NJ, Southgate TD, Klatzmann D, Lassmann H, Castro MG, Lowenstein PR. Chronic brain inflammation and persistent herpes simplex virus 1 thymidine kinase expression in survivors of syngeneic glioma treated by adenovirus-mediated gene therapy: implications for clinical trials. Nat Med 1999;5:1256–1263. [PubMed: 10545991]

77. Candolfi M, Curtin JF, Xiong W, Kroeger KM, Liu C, Rentsendorj A, Agadjanian H, Medina-Kauwe L, Palmer D, Ng P, Lowenstein PR, Castro MG. Effective high capacity gutless adenoviral vectors mediated transgene expression in human glioma cells. Mol Ther 2006;14:371–381. [PubMed: 16798098]

78. Maleniak TC, Darling JL, Lowenstein PR, Castro MG. Adenovirus-mediated expression of HSV1-TK or Fas ligand induces cell death in primary human glioma-derived cell cultures that are resistant to the chemotherapeutic agent CCNU. Cancer Gene Ther 2001;8:589–598. [PubMed: 11571537]

79. Albert FK, Forsting M, Sartor K, Adams HP, Kunze S. Early postoperative magnetic resonance imaging after resection of malignant glioma: objective evaluation of residual tumor and its influence on regrowth and prognosis. Neurosurgery 1994;34:45–60. [PubMed: 8121569]discussion 60–61

80. Choucair AK, Levin VA, Gutin PH, Davis RL, Silver P, Edwards MS, Wilson CB. Development of multiple lesions during radiation therapy and chemotherapy in patients with gliomas. J Neurosurg 1986;65:654–658. [PubMed: 3021931]

81. Assanah M, Lochhead R, Ogden A, Bruce J, Goldman J, Canoll P. Glial progenitors in adult white matter are driven to form malignant gliomas by platelet-derived growth factor-expressing retroviruses. J Neurosci 2006;26:6781–6790. [PubMed: 16793885]

82. Pena L, Perez-Alenza MD, Rodriguez-Bertos A, Nieto A. Canine inflammatory mammary carcinoma: histopathology, immunohistochemistry and clinical implications of 21 cases. Breast Cancer Res Treat 2003;78:141–148. [PubMed: 12725414]

83. Mahapokai W, Van Sluijs FJ, Schalken JA. Models for studying benign prostatic hyperplasia. Prostate Cancer Prostatic Dis 2000;3:28–33. [PubMed: 12497158]

84. Ahrar K, Madoff DC, Gupta S, Wallace MJ, Price RE, Wright KC. Development of a large animal model for lung tumors. J Vasc Interv Radiol 2002;13:923–928. [PubMed: 12354827]

85. Dickerson EB, Fosmire S, Padilla ML, Modiano JF, Helfand SC. Potential to target dysregulated interleukin-2 receptor expression in canine lymphoid and hematopoietic malignancies as a model for human cancer. J Immunother 2002;25:36–45. [PubMed: 11924909]

86. Vail DM, MacEwen EG. Spontaneously occurring tumors of companion animals as models for human cancer. Cancer Invest 2000;18:781–792. [PubMed: 11107448]
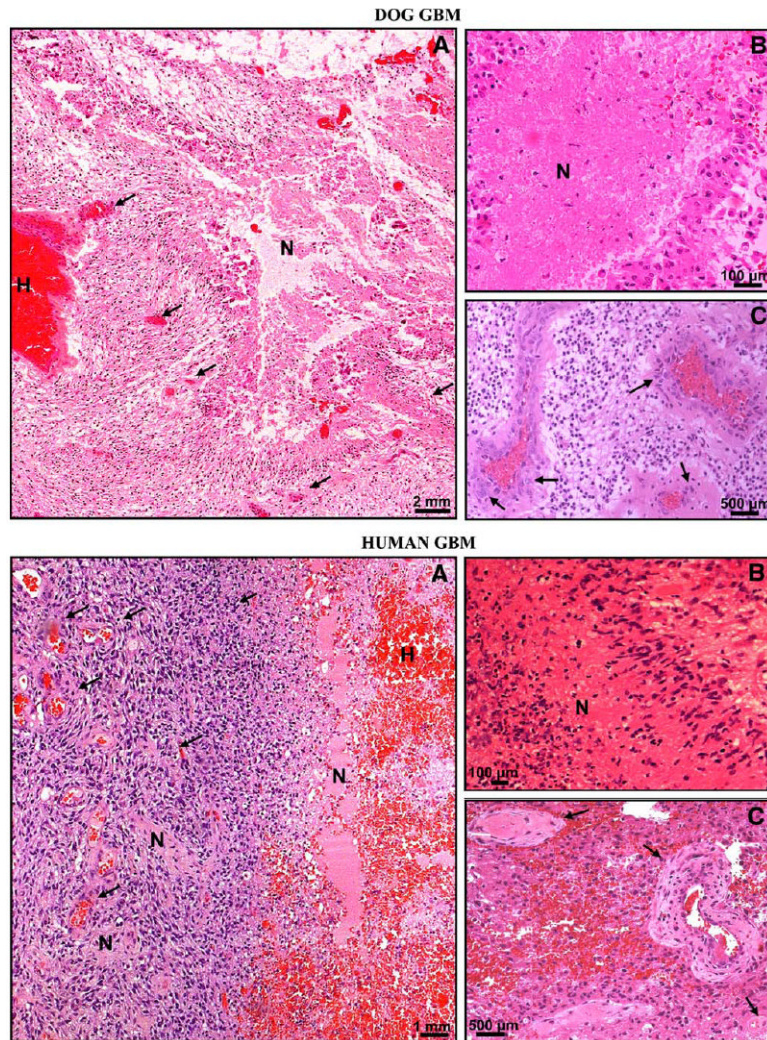
Fig. 1.
Histopathological comparisons between dog (*top panels*) and human (*bottom panels*) spontaneous GBM. Paraffin sections (5 μm) of spontaneous human and canine GBM were stained with hematoxylin and eosin (*H–E*) to determine their histopathologic features. **a** Low-magnification microphotographs show multiple areas of necrosis and profuse hemorrhages in both tumors. There are prominent necroses, serpentine pseudopalisading, thrombosed tumor vessels, and microvascular/endothelial proliferation in human and dog GBMs. *H* hemorrhage, *N* necrosis. *Arrows* indicate blood vessels. **b** High-magnification microphotographs show necrotic foci surrounded by pseudopalisading in human and dog GBMs. *N* necrosis. **c** High-magnification microphotographs demonstrate microvascular/endothelial proliferation in human and dog GBM. *Arrows* show tumoral blood vessels exhibiting endothelial proliferation
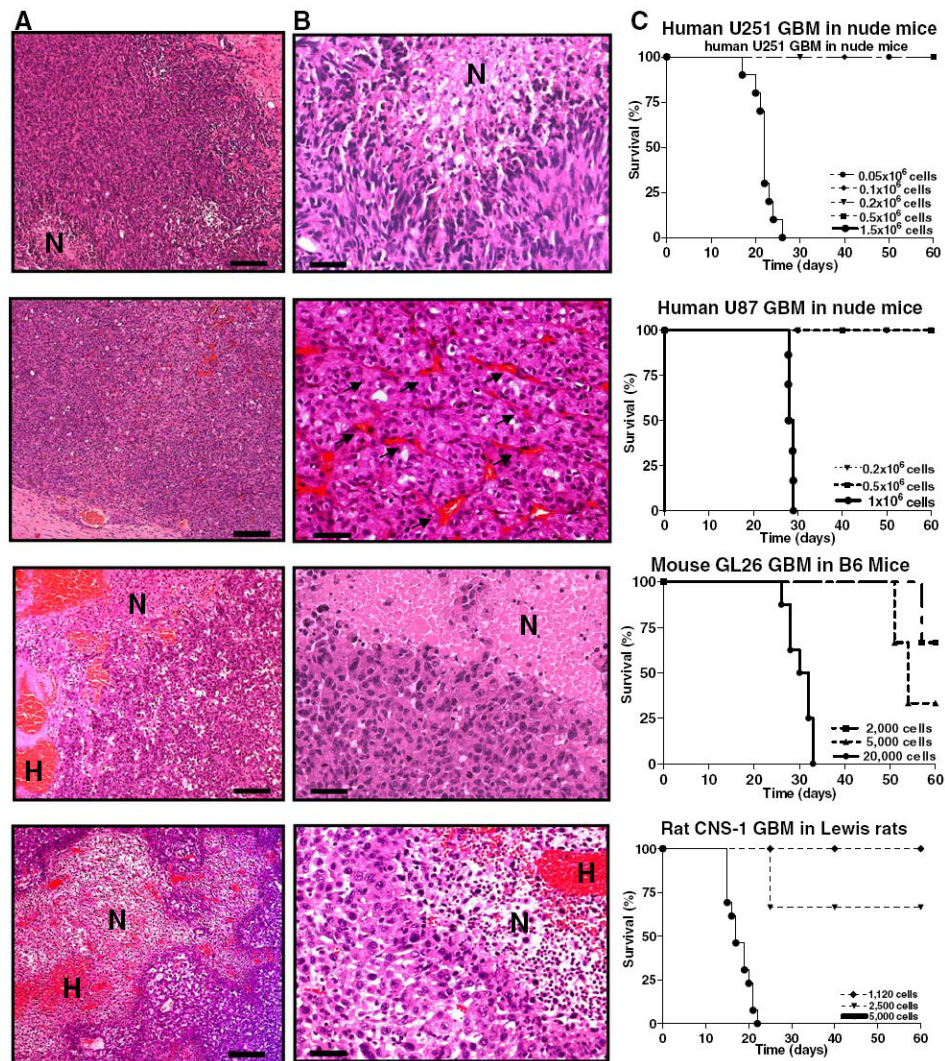
Fig. 2.
Histopathological comparisons amongst syngeneic rodent GBM models (CNS-1 in Lewis rat and GL26 in C57/B6 mouse) and human GBM xenografts in nude mice (U251 and U87). Paraffin sections (5 μm) of rat CNS-1 and mouse GL26 syngeneic gliomas, and U251 and U87 human xenografts in nude mice were stained with hematoxylin and eosin (*H–E*) to determine their histopathological features. **a** Low-magnification microphotographs show multiple areas of necrosis and profuse hemorrhages in all the tumors, with the exception of U87 xenografts. *Scale bar* 1 mm. *H* hemorrhage, *N* necrosis. **b** High-magnification microphotographs represent necrotic foci seen in GBM from all species. The pseudopalisading surrounding necrotic foci as in human GBM is found in CNS-1 GBMs and human U251 tumors, while GL26 GBM in mice exhibit necrotic foci surrounded by a rim of tumoral cells. U87 xenografts do not exhibit necrosis as a typical feature, but they show profuse neovascularizarion (*arrows*). *Scale bar* 100 μm. *N* necrosis. **c** Typical survival curves of the rodent GBM models (CNS-1 in Lewis rat: *n* = 13; GL26 in C57/B6 mouse: *n* = 8; U251 human GBM xenografts in nude mice: *n* = 10; U87 human GBM xenografts in nude mice: *n* = 6)
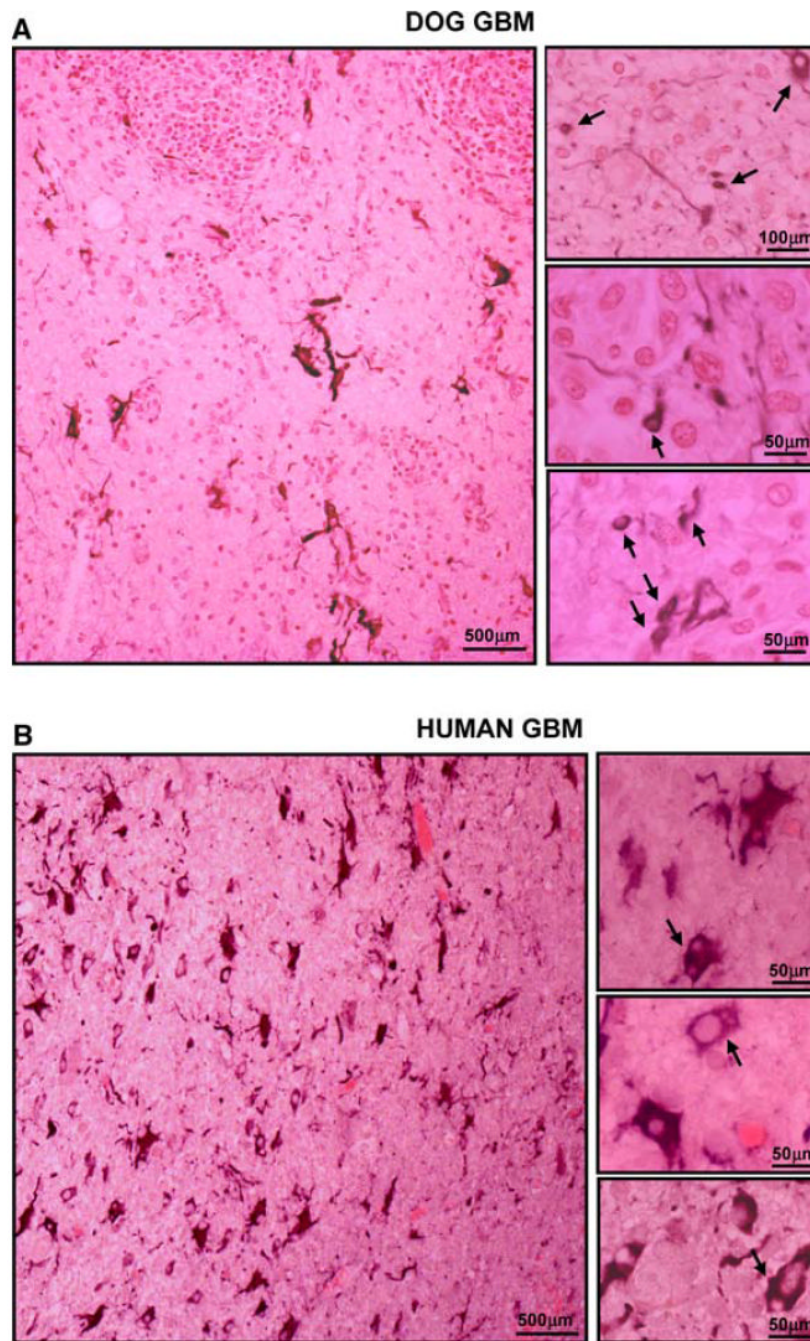
Fig. 3.
Neoplastic cellular infiltration into surrounding non-neoplastic brain tissue in spontaneous canine (**a**) and human GBMs (**b**). Paraffin sections (5 μm) from dog and human GBMs were stained with with GFAP antibodies. The microphotographs show that several of the small rounded cells infiltrating the non-neoplastic brain parenchyma express GFAP
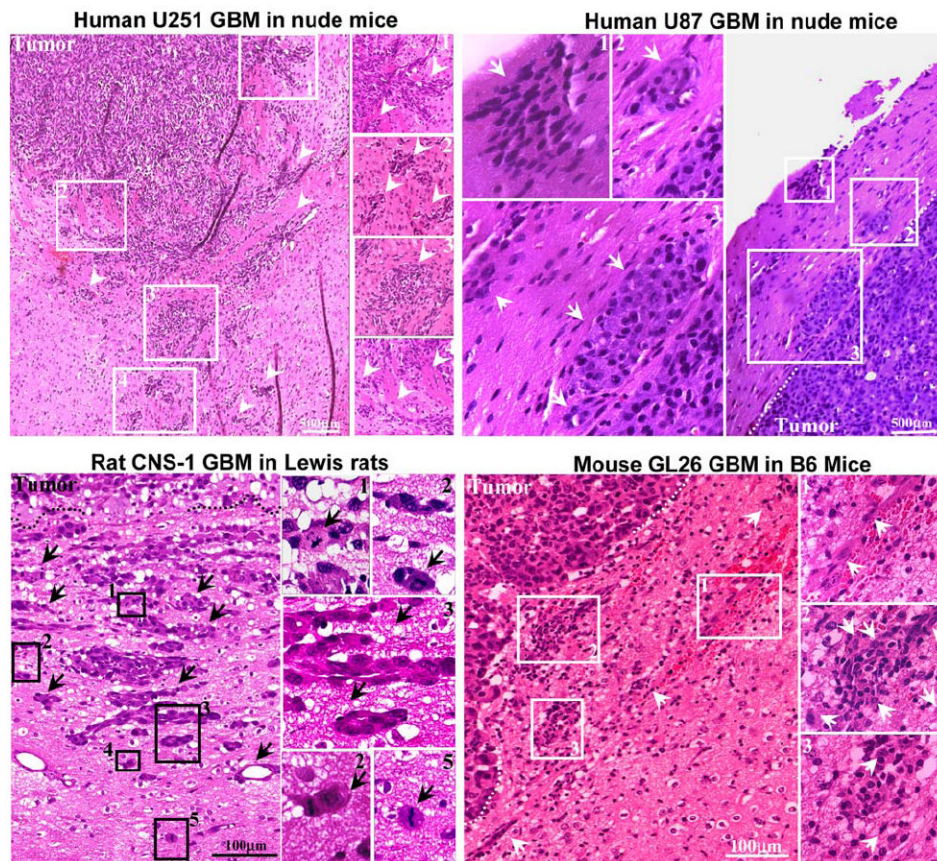
Fig. 4.
Neoplastic cellular infiltration into surrounding non-neoplastic brain tissue in syngeneic rat (CNS-1) and mouse (GL26) GBM models and human glioma xenografts in nude mice (U251 and U87). Paraffin sections (5 μm) from GBM were stained with hematoxylin and eosin for evaluating neoplastic invasion. The numbers in low-magnification microphotographs depict areas magnified in the microphotographs on the right. *Arrows* indicate malignant cells, clusters of GBM cells, and tumoral blood vessels infiltrating surrounding brain parenchyma. The indistinct tumor borders and the malignant cells clearly entering the non-neoplastic brain tissue suggest an invasive phenotype
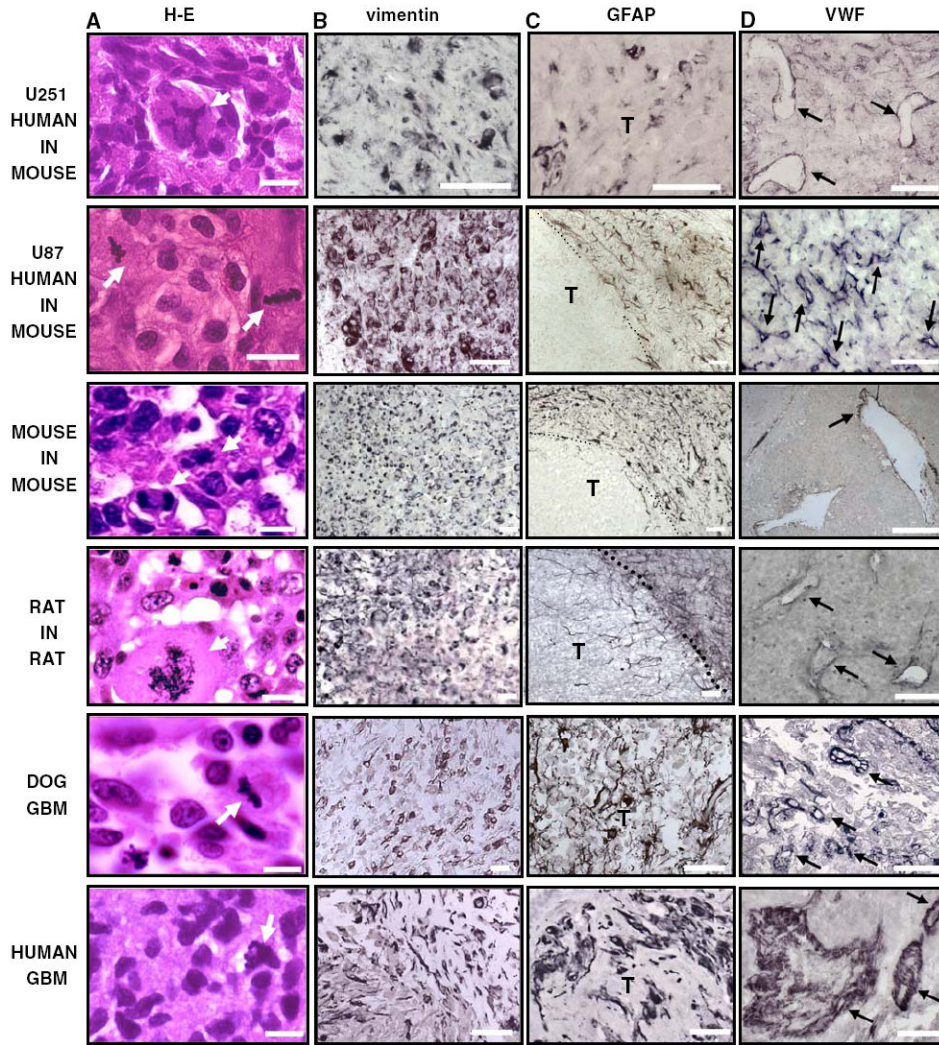
Fig. 5.
Cellular composition of human and dog spontaneous GBM, syngeneic rat (CNS-1) and mouse (GL26) GBM models and human glioma xenografts in nude mice (U251 and U87). Paraffin sections (5 μm) were obtained from spontaneous human and canine GBM as well as rat CNS-1 and mouse GL26 syngeneic gliomas and U251 and U87 human xenografts in nude mice. **a** GBM sections were stained with hematoxylin and eosin (*H–E*). High-magnification microphotographs show nuclear atypia and cell pleomorphism in human, dog, and murine GBM. *Scale bar* 25 μm. *Arrows* indicate aberrant mitotic figures. **b–c** Expression of astrocytic intermediate filaments, vimentin, and glial fibrillary astrocytic protein (*GFAP*), were detected in GBM sections by immunocytochemistry. *T* tumor. *Scale bar* 100 μm. **d** The expression of the endothelial marker Von Willebrand Factor (*VWF*) was detected in the blood vessels of human, dog and murine GBM sections by immunocytochemistry. *Arrows* indicate some of the blood vessels expressing VWF. *Scale bar* 250 μm
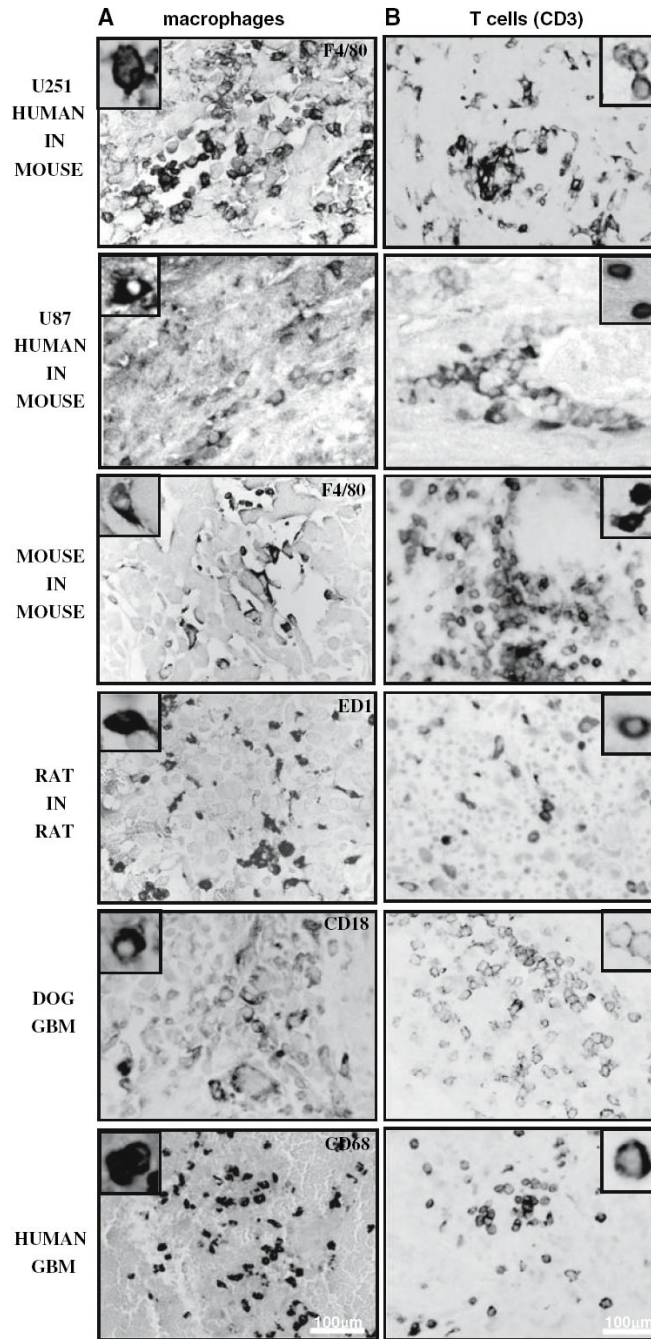
Fig. 6.
Immune/inflammatory infiltration in human glioblastoma, spontaneous GBM in dogs, syngeneic rat (CNS-1) and mouse (GL26) models and human glioma xenografts in nude mice (U251 and U87). **a** Inflammatory cells' infiltration was analyzed using paraffin sections (5 μm) from spontaneous human and canine GBM as well as rat CNS-1 and mouse GL26 syngeneic gliomas and U251 and U87 human xenografts in nude mice. **a** Human, dog, rat, and mouse macrophages were identified using antibodies against CD68, CD18, CD68 ED1, and F4/80, respectively. Insets show high-magnification microphotographs of positive cells. CD3ε cells were detected using specie-specific antibodies against CD3. Insets show high-magnification microphotographs of macrophages and CD3-positive cells

Table 1

Characteristic histological features present in human GBM, intracranial xenograft, and syngeneic rodent GBM models and dog spontaneous GBM

Histological features	Human	Dog	Rat	Mouse	U251 Human in mouse	U87 Human in mouse
Astrocytic intermediate filaments expression	GFAP/vimentin	GFAP/vimentin	Vimentin	Vimentin	GFAP/vimentin	Vimentin
Necrosis, hemorraghes	+	+	+	+	+	−
Pseudopalisading	+	+	+	+/−	+	−
Angiogenesis/neovascularization	+	+	+	+	+	+
Endothelial proliferation	+	+	−	−	−	−
Invasion	+	+	+/−	+/−	+/−	+/−
Hypercellularity, pleomorphism, and nuclear atypia	+	+	+	+	+	+
Inflammation	+	+	+	+	+	+

Table 2

Biological features of intracranial xenograft and syngeneic rodent GBM models and spontaneous GBM in dogs

Tumor biology	Dog	Rat	Mouse	Human in mouse
Tumor stablishment	Spontaneous	Syngenic	Syngeneic	Xenograft
Survival rates when non treated	1–2 months after diagnosis	~15 days after implantation	~30 days after implantation	~3–4 weeks after implantation
Allows study of anti-tumoral immune responses	+	+	+	−
Allows study of human-targeted therapies	−	−	−	+
Allows In vivo imaging	+	+	+	+
Reproducible tumor growth rates	−	+	+	+/−
Similar time to death of animals	−	+	+	+
Availability	+/−	+	+	+
Cost	High	Low	Low	Low
Allows to evaluate large number of animals	+/−	+	+	+